GENERALIZED YUV INTERPOLATION OF CFA IMAGES

Meng Wang and Thierry Blu

The Chinese University of Hong Kong
Department of Electronic Engineering
Shatin, New Territories, Hong Kong S. A. R.
{s065928, tblu}@ee.cuhk.edu.hk

ABSTRACT

This paper presents a simple yet effective color filter array (CFA) interpolation algorithm. It is based on a linear interpolating kernel, but operates on YUV space, which results in a nontrivial boost on the peak signal-to-noise ratio (PSNR) of red and blue channels. The algorithm can be implemented efficiently. At the end of the paper, we present its performance compared with nonlinear interpolation methods and show that it's competitive even among state-of-the-art CFA demosaicing algorithms.

Index Terms— color filter array, interpolation, linear kernel, YUV

1. INTRODUCTION

Most digital cameras capture color images using a single, monochrome sensor. The sensor is covered by a color filter array (CFA) such that incoming light is spectrally sampled. Due to the presence of the CFA, only one of R, G and B components is sampled at each pixel sampling location, resulting (together with other information) in the image known as the raw image. The most popular type of such mosaic is Bayer Filter Array [1], shown in figure 1.

The raw image undergoes a chain of processing stages inside the digital camera before finally presented as a full-color image. One of the most important stages is demosaicing, in which the missing color components at each pixel are estimated using some prior knowledge.

Demosaicing can be essentially formulated as an upsampling problem. The real image is first downsampled by the camera and then upsampled in the demosaicing process. Therefore, standard interpolation techniques such as bilinear interpolation can be directly applied. Such techniques are fast, memory-saving, but are subject to non-negligible artifacts such as false color and zipper effect [14]. They are primarily consequences of bad sampling and ringing effect across edges.

Nonlinear methods make use of spatial and interchannel correlation to help restoration. State-of-the-art restoration
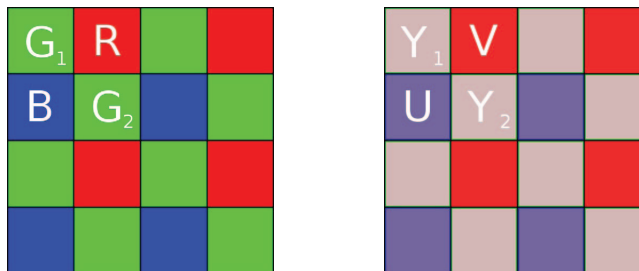

Fig. 1. Left: A typical Bayer color filter array configured as G R (first row), B G (second row) pattern for every 2×2 patch. The component indicated at each pixel is captured by the camera. Right: Sampling assumption for the YUV components. The goal is to use this assumption to interpolate Y, U and V consistently with the layout of RGB sampled values.

techniques include smooth hue transition [14] [2] and edge-directed interpolation [4] [15]. They achieve excellent results in terms of peak signal-to-signal ratio (PSNR).

To our knowledge, all the state-of-the-art techniques mentioned make use of RGB information exclusively. We propose a new vision on demosaicing, with linear interpolating kernels, but in the YUV space. Although the PSNR obtained does not outperform all the techniques above on standard test images (lighthouse 1, lighthouse 2, sails, buildings) in this realm of research, we obtain a boost in the R and B channels (about 5 dB) for almost free (no prior knowledge on hue or edges is assumed). The linear interpolating kernels we experimented include B-spline family functions and O-MOMS functions.

2. COLOR FILTER ARRAY INTERPOLATION

2.1. Traditional Approach

Bayer color filter array samples in such a way that the number of samples in G channel double those in R and B channels respectively. The reason is based on human visual system, the luminance response of which peaks at around the frequency of green light.

Bayer color filter array is defined in figure 1. We define $\mathbf{e}_1 = \begin{bmatrix} 1 \\ 0 \end{bmatrix}$ and $\mathbf{e}_2 = \begin{bmatrix} 0 \\ 1 \end{bmatrix}$. The samples captured by the camera can be represented as

$$\mathbf{S}^{\text{sample}}(\mathbf{n}) = \begin{bmatrix} R'(\mathbf{n}) \\ G_1'(\mathbf{n}) \\ G_2'(\mathbf{n}) \\ B'(\mathbf{n}) \end{bmatrix} = \begin{bmatrix} R(\mathbf{Dn} + \mathbf{e}_2) \\ G(\mathbf{Dn}) \\ G(\mathbf{Dn} + \mathbf{e}_1 + \mathbf{e}_2) \\ B(\mathbf{Dn} + \mathbf{e}_1) \end{bmatrix}. \qquad (1)$$

Standard interpolation is based on Shannon sampling and reconstruction theorem. The reconstructed R channel from a downsampled image $R'(\mathbf{n})$, for example, can be expressed as a convolution of samples and the sinc function $R^{\text{int}}(\mathbf{r}) = \sum_{\mathbf{k}} R'(\mathbf{k}) \text{sinc}(\mathbf{D}^{-1}(\mathbf{r} - \mathbf{e}_2) - \mathbf{k})$, where $\mathbf{r}$ represents a continuous coordinate and we use the exponent "int" to indicate the interpolated (rather than the real) value. $\mathbf{D}$ is the upsampling matrix $\begin{bmatrix} 2 & 0 \\ 0 & 2 \end{bmatrix}$.

Furthermore, generalized interpolation [9] [6] allows us to use more generalized kernel functions $\varphi(\mathbf{r})$ in lieu of the sinc function and a sequence of generalized samples $c_{\text{R}}(\mathbf{k})$ instead of the captured samples $R'(\mathbf{k})$.

With generalized interpolation, a family of kernels based on B-spline functions can be used [7]. A B-spline function β^m of degree m is defined by its Fourier transform $\hat{\beta}^m(\omega) = \left(\frac{\sin(\omega/2)}{\omega/2}\right)^{(m+1)}$. Nearest-neighbor and bilinear interpolations correspond to β^0 and β^1 kernels, respectively.

The hypothesis for R channel can thus be formulated as

$$R^{\text{int}}(\mathbf{r}) = \sum_{\mathbf{k}} c_{\text{R}}(\mathbf{k}) \varphi(\mathbf{D}^{-1}(\mathbf{r} - \mathbf{e}_2) - \mathbf{k}) \qquad (2)$$

where φ is an arbitrary good approximation kernel function satisfying properties described in [9]. The superscript int indicates that the image is interpolated rather than given. Examples of those functions include B-spline functions [7] and O-MOMS functions [12].

2.2. Choice of Color Space

The main disadvantage of RGB representation is the high correlation between its components. Tkalcic [5] reported that there is a 0.78 for τ_{BR} (cross correlation between B and R), 0.98 for τ_{RG} and 0.94 for τ_{GB}.

RGB is HVS based, and RGB devices have a luminance response similar to figure 2, from which we observe a substantial channel overlap. Therefore, it is very likely that interpolating them separately and ignoring the interchannel correlation may not produce a "good" result. For this reason, it is desirable to look for alternative color spaces in which each component is isolated from the others.

2.3. New Prior Based on Alternative Color Space

An example of such a color space representation is the YUV color space. Our rationale is that this color space is characterized by a luminance (Y) component and two chrominance (U
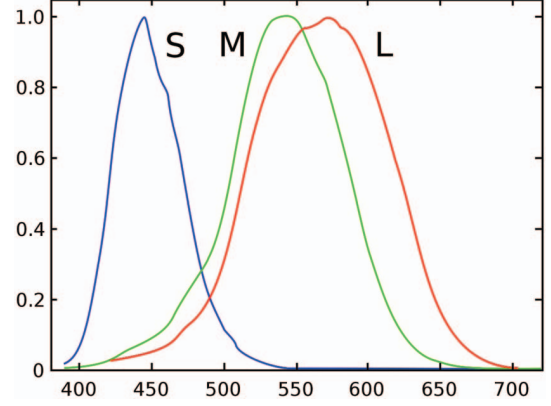

Fig. 2. Human visual system response to luminance. There are three types of cone cells, and two of them concentrate on green-yellow color band.

and V) components. The three components are less correlated in the sense that luminance and chrominance components are separated explicitly on the CFA [3]. Luminance component accounts for light intensity, whereas chrominance components are differential components used to discriminate colors. For example, R can be obtained by subtracting a weighted chrominance component (V) from the luminance component. RGB space is related to YUV space by a linear transformation matrix $[1, 0, 1.13983; 1, -0.39465, -0.5806; 1, 2.03211, 0]$. Based on the new color space, we make a new hypothesis in a similar fashion to the one in RGB space:

- Y can be represented with its samples on the quincunx grid where G is sampled.

- U and V can be represented with samples on the interlacing grids respectively where B and R are sampled.

Now, we adapt equation 2 to our new hypothesis:

$$Y_1^{\text{int}}(\mathbf{r}) = \sum_{\mathbf{k}} c_{\text{Y1}}(\mathbf{k}) \varphi(\mathbf{D}^{-1}\mathbf{r} - \mathbf{k})$$
$$Y_2^{\text{int}}(\mathbf{r}) = \sum_{\mathbf{k}} c_{\text{Y2}}(\mathbf{k}) \varphi(\mathbf{D}^{-1}(\mathbf{r} - \mathbf{e}_1 - \mathbf{e}_2) - \mathbf{k})$$
$$U^{\text{int}}(\mathbf{r}) = \sum_{\mathbf{k}} c_{\text{U}}(\mathbf{k}) \varphi(\mathbf{D}^{-1}(\mathbf{r} - \mathbf{e}_1) - \mathbf{k})$$
$$V^{\text{int}}(\mathbf{r}) = \sum_{\mathbf{k}} c_{\text{V}}(\mathbf{k}) \varphi(\mathbf{D}^{-1}(\mathbf{r} - \mathbf{e}_2) - \mathbf{k}). \qquad (3)$$

The hypothesis can also be represented as matrix form

$$\mathbf{T}^{\text{int}}(\mathbf{r}) = \sum_{\mathbf{k}} \mathbf{\Phi}(\mathbf{D}^{-1}\mathbf{r} - \mathbf{k})\mathbf{\Gamma}(\mathbf{k}) \qquad (4)$$

where $\mathbf{\Phi}$ is a 4×4 diagonal matrix, and we define

$$\mathbf{T}^{\text{int}}(\mathbf{r}) = \begin{bmatrix} Y_1^{\text{int}}(\mathbf{r}) & Y_2^{\text{int}}(\mathbf{r}) & U^{\text{int}}(\mathbf{r}) & V^{\text{int}}(\mathbf{r}) \end{bmatrix}^{\text{T}}$$

$$\mathbf{\Gamma}(\mathbf{k}) = \begin{bmatrix} c_{\text{Y1}}(\mathbf{k}) & c_{\text{Y2}}(\mathbf{k}) & c_{\text{U}}(\mathbf{k}) & c_{\text{V}}(\mathbf{k}) \end{bmatrix}^{\text{T}}$$
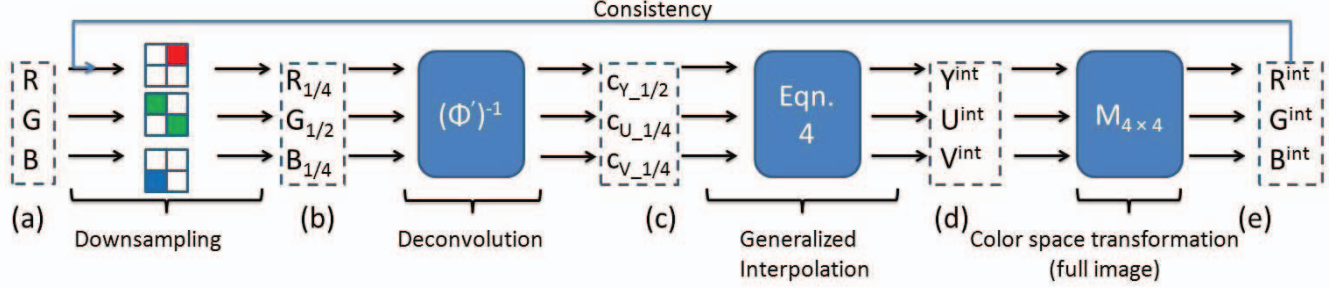
Fig. 3. Flowchart of the sampling and reconstruction process. Note that the interpolated image is consistent with the full-color unknown image on samples captured by the camera. (a) Full-color unknown image; (b) CFA image captured by camera; (c) Generalized YUV samples; (d) Interpolated full-color image in YUV representation; (e) Reconstructed RGB image.

.
We relate equation 4 to the RGB samples captured by the camera. A 4×4 version of transformation matrix $\mathbf{M}_{4\times4} =$
$\begin{bmatrix} 1 & 1 & 0 & 1.13983 \\ 1 & 1 & -0.39465 & -0.5806 \\ 1 & 1 & -0.39465 & -0.5806 \\ 1 & 1 & 2.03211 & 0 \end{bmatrix}$ by first replicating the first
column, and then the second row.

$$\begin{bmatrix} R^{\text{int}}(\mathbf{r}) \\ G_1^{\text{int}}(\mathbf{r}) \\ G_2^{\text{int}}(\mathbf{r}) \\ B^{\text{int}}(\mathbf{r}) \end{bmatrix} = \sum_{\mathbf{k}} \mathbf{M}_{4\times4} \Phi(\mathbf{D}^{-1}\mathbf{r} - \mathbf{k})\Gamma(\mathbf{k}) \quad (5)$$

3. DECONVOLVING AND INTERPOLATION

In order to perform the interpolation in equation 5, the coefficients in $\Gamma(\mathbf{k})$ must be found at first. This process is essentially a deconvolution operation.
Substitute the captured samples in equation 1 to obtain

$$\mathbf{S}^{\text{sample}}(\mathbf{n}) = \sum_{\mathbf{k}} \Phi'(\mathbf{n} - \mathbf{k})\Gamma(\mathbf{k}). \quad (6)$$

where $\Phi'(\mathbf{k})$ can be obtained directly from the sampled values of $\mathbf{M}_{4\times4}\Phi(\mathbf{r})$. This equation can be solved efficiently by using DFT and solving a linear system in the Fourier domain. The step corresponds to the stage between (b) and (c) in figure 3.
Finally, the full image in YUV representation (figure 3 (d)) can be interpolated with equation 3. The RGB image is obtained using the color space transformation matrix $\mathbf{M}_{4\times4}$.

4. EXPERIMENTS AND RESULTS

The algorithm is implemented with MATLAB. We test our algorithm by first applying the Bayer filter to a full color test image, mimicking the capturing operation in the digital camera, and then demosaicing the sampled image. For a 768 by 512 image, it takes about 1 second to reconstruct using β^3 kernel. We use Peak Signal-to-Noise Ratio (PSNR) as the metric for the demosaicing quality. The PSNR between the original image for reference $\mathbf{I}_{\text{ref}}$ and the reconstructed image $\mathbf{I}_{\text{cmp}}$ for a certain channel is given by

$$\text{PSNR} = 10 \cdot \log_{10}\left(\frac{(\max(\max(\mathbf{I}_{\text{ref}})))^2}{\frac{1}{mn}\sum\sum||\mathbf{I}_{\text{ref}} - \mathbf{I}_{\text{cmp}}||^2}\right) \quad (7)$$

where mn is the total number of pixels in the image.
We tested the algorithm over a wide range of kernels, including β^0 through β^5 and O-MOMS functions φ_o^0 through φ_o^5, which generally outperforms the B-spline kernel of the same degree [11] [12]. Increasing the kernel degree does not affect the processing time significantly. Some of the representative results are tabulated in tables 1.
We observe a nontrivial improvement on PSNR with linear interpolation in YUV space, for any interpolating kernel, by 3 $\sim$ 5 dB in R and B PSNRs. However, the G PSNR is actually a little bit smaller than if interpolated in RGB space. Nevertheless, the loss is tolerable. The loss can be compensated by performing another interpolation in the G channel using prior in equation 2 and swapping it back to the reconstructed image.
Since the interpolation is done in Fourier space, very little adaptive step could be applied within the process. It is our ongoing project to apply a nonlinear post-processing step (such as [14]) to improve the quality in artifact prone regions such as edges.

5. CONCLUSIONS AND DISCUSSIONS

We present an efficient algorithm for demosaicing a Bayer image in YUV space with a linear kernel function, which significantly improves the quality of blue and red channels. The generalized linear interpolation can be used as a basis for more sophisticated, nonlinear techniques, such as median filtering [13] or alternating projections [2] [16]. When a 3×3 median filter is applied to the U and V channels in the reconstructed image, the PSNR of G channel increases by about 0.7 dB, and 0.3 dB for R and B channels (on lighthouse 1).

	B-spline 1 (bilinear)		B-spline 3		O-MOMS 3	
	RGB	YUV	RGB	YUV	RGB	YUV
Buildings	22.267	25.325	21.854	26.651	21.701	26.680
	27.280	26.126	29.764	29.372	29.870	29.594
	22.371	25.751	21.924	26.690	21.770	26.681
Lighthouse 1	26.811	30.132	26.590	31.765	26.450	31.815
	31.766	30.566	34.382	33.877	34.500	34.126
	26.999	30.739	26.686	31.999	26.554	31.984
Lighthouse 2	27.106	30.144	26.784	30.560	26.632	30.374
	31.339	29.952	32.811	32.224	32.784	32.358
	27.452	30.466	26.929	30.592	26.753	30.345
Sailboats	31.246	33.325	31.073	34.652	30.905	34.625
	34.936	33.752	37.359	36.884	37.444	37.097
	29.571	33.865	29.621	34.697	29.547	34.644

Table 1. PSNR for Interpolation results. Each cell shows in turn the PSNR for R, G and B channel.

Experiments on YUV-siblings such as YPbPr, YCbCr or YIQ reveal similar performance.

Having shown that YUV space is good for improving the demosaicing quality, we hypothesize that there exists a nonstandard color space that particularly leverages a certain channel. We are working in search of such a magic color space by modifying the linear transformation matrix $\mathbf{M}_{4\times 4}$.

6. REFERENCES

[1] B. E. Bayer, "Color Imaging Array", *United States Patent 3971065*, July 1976.

[2] Bahadir K. Gunturk, Yucel Altunbasak and Russell M. Mersereau, "Color Plane Interpolation Using Alternating Projections", *IEEE Transactions on Image Processing*, vol. 11, no. 9, 2002.

[3] D. Alleysson, S. Süsstrunk and J. Herault, "Linear demosaicing inspired by the human visual system". *IEEE Transactions on Image Processing*, vol. 14, no. 4, 439 – 449, April 2005.

[4] J. F. Hamilton Jr. and J. E. Adams, "Adaptive Color Plane Interpolation in Single Sensor Color Electronic Camera", *United States Patent 5629734*, May 1997.

[5] Marko Tkalcic and Jurij F. Tasic, "Colour Spaces - Perceptual, Historical and Applicational Background", *EUROCON Computer as a Tool*, vol. 1, 304 – 308, 2003.

[6] M. Unser, "Sampling - 50 Years After Shannon", *Proceedings of the IEEE*, Vol. 88, No. 4, April 2000.

[7] M. Unser, "Splines: A Perfect Fit for Signal and Image Processing", *IEEE Signal Processing Magazine*, 16:22 – 38, November 1999.

[8] Phillippe Thévenaz, Thierry Blu and Michael Unser, "Image Interpolation and Resampling", *Handbook of Medical Imaging*, 393 – 420, 2000.

[9] Phillippe Thévenaz, Thierry Blu and Michael Unser, "Interpolation Revisited", *IEEE Transactions on Medical Imaging*, vol. 19, no. 7, July 2000.

[10] Rastislav Lukac. *Single-Sensor Imaging: Methods and Applications for Digital Cameras*. CRC Press, Inc. Boca Raton, FL, USA. 2008.

[11] Thierry Blu, Philippe Thévenaz and Michael Unser, "Minimum Support Interpolators with Optimum Approximation Properties", *Proceedings of ICIP 1998*, Vol. 3, 242 – 245, October 1998.

[12] Thierry Blu, Philippe Thévenaz and Michael Unser, "MOMS: Maximal-Order Interpolation of Minimal Support", *IEEE Transactions on Image Processing*, Vol. 10, No. 7, July 2001.

[13] W. T. Freeman, "Median Filter for Reconstructing Missing Color Samples", *U.S. Patent 4724395*, 1988.

[14] Wenmiao Lu and Yap-Peng Tan, "Color Filter Array Demosaicking: New Method and Performance Measures", *IEEE Tran. on Image Proc.*, vol. 12, no. 10, 2003.

[15] Xin Li and Michael T. Orchard, "New Edge-Directed Interpolation", *IEEE Transactions on Image Processing*, vol. 10, no. 10, 2001.

[16] Yue M. Lu, M. Karzand and M. Vetterli, "Demosaicking by Alternating Projections: Theory and Fast One-Step Implementation". IEEE Transactions on Image Processing, vol. 19, no. 8, August 2010.